Eur. Phys. J. D **41**, 205–210 (2007)
DOI: 10.1140/epjd/e2006-00208-x

THE EUROPEAN PHYSICAL JOURNAL D

Laser polarization effects on K-shell Compton scattering

O. Budriga and V. Florescu[a]

Department of Physics, University of Bucharest, Bucharest-Magurele MG11, 077125, Romania

Received 10 April 2006 / Received in final form 3 August 2006
Published online 15 September 2006 –

Abstract. We study Compton scattering on the ground state of the hydrogen atom in the presence of an intense low-frequency electric field (the laser) of arbitrary polarization, for incident and scattered photons of energies around 15 keV. The adopted formalism is the nonrelativistic one developed by Voitkiv et al. [J. Phys. B: At. Mol. Opt. Phys. **36**, 1907 (2003)] and applied by them for a circularly polarized laser. We explore the spectrum and the electron energy distribution in their dependence on the incident photon energy or electric field intensity, for different polarizations.

PACS. 34.50.Rk Laser-modified scattering and reactions – 32.80.Wr Other multiphoton processes

1 Introduction

The progress in the laser performances in terms of intensity, spectral domain and pulse duration has increased the interest in the theoretical studies of matter interaction with intense external electromagnetic fields. Some of the most studied phenomena, like above-threshold ionization and high-order-harmonic generation, are new and were discovered in experiments using intense lasers. Another category of studied phenomena includes basic atomic processes, like electron-atom scattering, photoionization, bremsstrahlung and X-ray scattering, as modified by the presence of the laser.

We report here some new results concerning the case of Compton effect on an electron in the ground state of a hydrogenic atom with nuclear charge Z. Recent calculations [1,2] performed for the hydrogen atom have revealed a substantial influence of a low-frequency laser field on the K-shell Compton scattering, for laser intensities of the order 10^{-5} au.

In the usual Compton scattering on a bound electron, an incident photon with momentum $\boldsymbol{\kappa}_1$ and polarization vector $\mathbf{s}_1$ is inelastically scattered by the electron. As a result, a photon with the attributes $\boldsymbol{\kappa}_2$ and $\mathbf{s}_2$ is emitted and the electron leaves the atom with an asymptotic momentum $\mathbf{p}$. For a review of the theoretical description of the process see the paper of Bergstrom and Pratt [3]. If the atomic nucleus is fixed, energy is conserved but not the momentum. The usual description of the process concerns low intensity incident radiation, so it is based on perturbation theory. In a nonrelativistic treatment, justified for incident photon energy much lower than the electron rest energy, working in the velocity gauge, the transition amplitude is the sum of three terms. A first term, corresponding to the so-called "sea-gull" diagram, is the dominant one, if the incident photon energy is not too close to the ionization threshold. If the scattered photon energy is very low, an infrared divergence is present in another term of the amplitude. In the particular case of a hydrogenic atom, it is possible to derive analytic expressions for all three terms in the transition amplitude; this was done many years ago for both K [4] and L-subshells [5], and later for any ns subshell [6].

In the literature, more attention was given to radiation scattering on free electrons than on bound ones, and particularly to *induced Compton scattering*, when the electron interacts only with one external monochromatic field (the laser), so the scattered radiation frequency spectrum is directly connected with the laser frequency. Both relativistic and nonrelativistic calculations are available in this case (for a recent calculation and references see the paper of Panek et al. [7]).

In *laser assisted* Compton scattering the electron interacts with two external field, one, of frequency ω_1, has low intensity and the other (the laser) is intense. The laser frequency ω_{L} is orders of magnitude lower than the frequency ω_1. In this case, although hundreds of laser photons are exchanged, the scattered radiation spectrum is dominated by frequencies in the range of ω_1.

Earlier considerations on laser assisted Compton scattering are connected with the papers of Jain et Tsoar [8] and Ehlotzy [9]. In the first part of their paper Jain and Tsoar consider the case of laser assisted X-ray scattering on a K-shell electron of a hydrogenic atom. They use the impulse approximation, a usual approximation for Compton scattering in the absence of the field [10], and

[a] e-mail: flor@barutu.fizica.unibuc.ro

neglect the modification of the ground state, except the energy shift. Ehlotzky's analysis is based on the contribution of the sea-gull term and includes laser effects on initial and final states using for both superpositions of Volkov states with the same momentum distribution as in the absence of the laser field.

New analytic and numerical results have been presented recently by Voitkiv et al. [1,2] for an electron bound in the K-shell of a hydrogen atom interacting with a circularly polarized laser. As in the work presented here, we have adopted Voitkiv et al. approach (designed in the following as VGU), details on it are given in Section 2. The mentioned authors have studied the fully differential spectra of emitted electrons and scattered photons in coincidence, the energy spectrum of the electrons for the case in which the scattered photons are not detected and the energy spectrum of the scattered photons for the case in which the electrons are not recorded. They have found that the dressing of the ground state plays an important role in the scattering pattern. All the results presented by Voitkiv et al. correspond to a photon energy $\hbar\omega_1 = 750$ au ≈ 20.4 keV.

As in the absence of the laser field, the sea-gull term vanishes in the dipole approximation, the retardation effects are included for the incident and scattered photon. Their energies should not be too small, for two reasons: (i) near the K-shell threshold the other two terms of the amplitudes do contribute, (ii) at low scattered frequency the infrared divergence shows up, in a term not included here.

After describing the formalism, we present at the end of Section 2 the expression (3) of the most differential cross-section for laser assisted Compton scattering in the case of arbitrary laser polarization. Some more details and further approximations are given in Section 3.

In Section 4 we present numerical results for hydrogen. We focus on the dependence on polarization for both the fully differential electron spectrum and the electron energy distribution. Particularly, we compare linear and circular polarization effects. We investigate several aspects not discussed by Voitkiv et al. [1,2], such as the dependence on the initial photon frequency and laser electric field intensity of the electron energy distribution.

In the analytic expressions we use SI units. The electron mass and charge are denoted by m_e and e ($e < 0$), respectively. The numerical results are discussed using atomic units for the parameters.

2 The theoretical framework

The approximation scheme developed by VGU [1] is a nonrelativistic treatment of the electron interaction with the electromagnetic radiation, which has a component described as a quantized field, responsible for the absorption of the incident photon and the spontaneous emission of the Compton photon, and a component described classically, which is brought by the laser and that modifies the features of the Compton effect. Retardation is included for the quantized field, but not for the laser. The Hamiltonian is written in the velocity gauge and the electron interaction with the quantized electromagnetic field, described by a potential vector operator $\hat{\mathbf{A}}$, is treated as a perturbation. The transition amplitude is of second order in this operator. Only the contribution of the sea-gull term (the $\hat{\mathbf{A}}^2$ term) is included.

In order to keep a connection with the previous work in [1], we refer to the same particular reference frame, with units vectors $\mathbf{e}_j$, $j = 1, 2, 3$ in a special relation with the laser field: $\mathbf{e}_2$ is along the propagation direction and the other two vectors along the principal axes of the ellipse described by the electric field. We use the vector potential

$$\mathbf{A}_{\mathrm{L}}(t) = A_0[\cos(\xi/2)\cos(\omega_{\mathrm{L}}t)\mathbf{e}_3 - \sin(\xi/2)\sin(\omega_{\mathrm{L}}t)\mathbf{e}_1], \tag{1}$$

which means that the polarization is described by the parameter ξ with $0 \leq \xi \leq \pi$. The amplitude of the electric field is $F_0 = \omega_{\mathrm{L}}A_0$. We have to remark that, due to a different factor in the expression of the vector potential, a calculation of ours for a given F_0 should agree with a calculation of [1] performed for $F_0\sqrt{2}$. This refers, of course, to the circularly polarized case, the only case considered in [1].

We adopt the same approximations as Voitkiv et al. for the dressed states of the bound and of the final electron, i.e., in the velocity gauge, the laser effect on the ground state is reduced to the multiplication by $\exp[\frac{ie}{\hbar}\mathbf{A}_{\mathrm{L}}(t)\cdot\mathbf{r}]$ of the bound state wavefunction and the final state is taken as a Coulomb−Volkov state. Arguments in favor of the approximation used for the ground state were presented by Voitkiv and Ullrich [11]. The Coulomb-Volkov function is obtained from the nonrelativistic Volkov solution by replacing the plane wave by a Coulomb scattering solution, denoted here by $|\mathbf{p}-\rangle$. The Coulomb-Volkov approximation was introduced by Jain and Tsoar [8]. Not long time after, Cavaliere et al. [12] have established a condition for its validity. In the appendix of their paper the equation satisfied by the Coulomb-Volkov function is compared with the exact time-dependent Schrödinger equation. The conclusion is that the inequality

$$\zeta \equiv \frac{F_0}{\omega_{\mathrm{L}}p} \ll 1 \tag{2}$$

has to be satisfied. A similar type of justification was given by Banerji and Mittleman [13]. A qualitative argument concerning the role of the electron energy comes from the simple remark that at large electron energies the Coulomb wavefunction becomes a plane wave and the Coulomb-Volkov wavefunction a Volkov solution.

The Coulomb-Volkov function is related to another approximate wave function introduced by Kroll and Watson [14] and used in low frequency calculations. This wave function was analyzed by Kornev and Zon [15], using as a test a relation, known as Siegert theorem, applied to one-photon free-free transitions. The calculation was done at low electron energies. For more details see [15][1].

[1] We owe the information about the calculation of Kornev and Zon to one of the referees of our paper.

The Volkov factor depends on the laser polarization and this leads to more complicate results if the polarization is not circular than otherwise. We give here the final results.

The most differential cross-section has the same structure as in the circularly polarized laser case (see [1], Eq. (14)),

$$d^4\sigma = \sigma_{\rm Th}\frac{\omega_2}{\omega_1}\hbar\sum_{n=-\infty}^{\infty}|M_{fi;n}|^2\delta(E_e+U_{\rm P}+n\hbar\omega_{\rm L} - E_1+\hbar\omega_2-\hbar\omega_1)dE_e d\Omega_e d\omega_2 d\Omega_2, \quad (3)$$

with $\sigma_{\rm Th}$ the Thomson cross-section. By E_e was denoted the asymptotic (kinetic) energy of the electron, by $U_{\rm P}$ the ponderomotive potential ($U_{\rm P}=e^2F_0^2/4m_e\omega_{\rm L}^2$) and by $E_1<0$ the bound electron energy. The expression of $M_{fi;n}$ depends on the laser polarization. In the general case its expression is

$$M_{fi;n} = \langle \mathbf{p}-|B_n(a,b;\Delta)e^{i(\boldsymbol{\kappa}_1-\boldsymbol{\kappa}_2)\cdot\mathbf{r}}|E_1\rangle, \quad (4)$$

with B_n the generalized Bessel function, as defined in [16]. The continuum energy eigenstate $|\mathbf{p}-\rangle$ is normalized in the energy and solid angle scales.

The exact expressions of the parameters a and Δ of the B_n function result from

$$a\cos\Delta = \frac{\alpha_0}{\hbar}[\mathbf{e}_3\cdot\mathbf{p}\cos(\xi/2)+m_e\omega_{\rm L}\mathbf{e}_1\cdot\mathbf{r}\sin(\xi/2)],$$
$$a\sin\Delta = \frac{\alpha_0}{\hbar}[\mathbf{e}_1\cdot\mathbf{p}\sin(\xi/2)-m_e\omega_{\rm L}\mathbf{e}_3\cdot\mathbf{r}\cos(\xi/2)], \quad (5)$$

while

$$b = \frac{U_{\rm P}}{2\hbar\omega_{\rm L}}\cos\xi. \quad (6)$$

We have used[2] the notation α_0 for the amplitude of the classical quiver motion of the electron in the external electric field of frequency $\omega_{\rm L}$, and linear polarization

$$\alpha_0 = -\frac{eF_0}{m_e\omega_{\rm L}^2}. \quad (7)$$

For the case of circularly polarized light ($\xi=\pi/2$), the parameter b vanishes and the generalized Bessel function becomes, up to a phase factor, the ordinary Bessel function $J_n(a)$. As said before, this is the only case studied in the two papers of Voitkiv et al.

All parameters b, a and Δ depend on the laser parameters, but a and Δ also depend on the electron momentum. The unpleasant feature is the dependence of the last two parameters on the integration variable $\mathbf{r}$ in (4).

3 Further details on the calculation

Based on the series expansion of the generalized Bessel functions (Ref. [16], Eq. (36)), the general expression (4) of $M_{fi;n}$ becomes a series whose terms are products of a Bessel function and a complicate matrix-element including another Bessel function,

$$M_{fi;n} = \sum_{m=-\infty}^{\infty}J_m(b)S_{nm},$$
$$S_{nm} \equiv \langle \mathbf{p}-|J_{n+2m}(a)\ e^{i[(n+2m)\Delta+(\boldsymbol{\kappa}_1-\boldsymbol{\kappa}_2)\cdot\mathbf{r}]}|E_1\rangle. \quad (8)$$

We emphasize that the expression of $M_{fi;n}$ contains only one matrix-element in the case of circular polarization, when $b=0$, while for other polarization cases one encounters a series of such matrix-elements.

As in the previously studied case, the atomic matrix elements are complicated by the $\mathbf{r}$-dependence of the parameters a and Δ. In the first paper of Voitkiv et al. one finds the justification for adopting approximate $\mathbf{r}$-independent expressions for a and Δ; the effects of the approximation, studied in their second paper, were found, with some exceptions, not to be essential. So, we adopt the same type of approximation, replacing a by the simpler $\mathbf{r}$-independent expression, denoted by $a^{(0)}$,

$$a^{(0)} = \frac{\alpha_0}{\hbar}[(\mathbf{e}_1\cdot\mathbf{p})^2\sin^2(\xi/2)+(\mathbf{e}_3\cdot\mathbf{p})^2\cos^2(\xi/2)]^{1/2}, \quad (9)$$

and Δ by

$$\Delta = \Delta^{(0)}+\Delta^{(1)}. \quad (10)$$

The value of $\Delta^{(0)}$ is extracted from

$$a^{(0)}\cos\Delta^{(0)} = \frac{\alpha_0}{\hbar}\mathbf{e}_3\cdot\mathbf{p}\cos(\xi/2),$$
$$a^{(0)}\sin\Delta^{(0)} = \frac{\alpha_0}{\hbar}\mathbf{e}_1\cdot\mathbf{p}\sin(\xi/2), \quad (11)$$

and Δ_1 is $\mathbf{r}$-dependent and it is proportional with the laser photon frequency

$$\Delta^{(1)} \approx -\mathbf{q}\cdot\mathbf{r},$$
$$\mathbf{q} \equiv m_e\omega_{\rm L}\frac{(\mathbf{e}_1\cdot\mathbf{p})\sin^2(\xi/2)\mathbf{e}_1+(\mathbf{e}_3\cdot\mathbf{p})\cos^2(\xi/2)\mathbf{e}_3}{(\mathbf{e}_1\cdot\mathbf{p})^2\sin^2(\xi/2)+(\mathbf{e}_3\cdot\mathbf{p})^2\cos^2(\xi/2)}. \quad (12)$$

With these approximations, the atomic matrix elements become

$$S_{nm} \approx S_{nm}^{(0)} = J_{n+2m}\left(a^{(0)}\right)\ e^{i(n+2m)\Delta^{(0)}}O_{nm},$$
$$O_{nm} = \langle \mathbf{p}-|e^{i[\boldsymbol{\kappa}_1-\boldsymbol{\kappa}_2-(n+2m)\mathbf{q}]\cdot\mathbf{r}}|E_1\rangle. \quad (13)$$

It was very useful for the numerical calculations to notice that the matrix elements O_{nm} have simple analytic expressions (see, for instance, Eq. (23) of [4]). With the notations

$$\lambda = \alpha Z m_e c, \qquad \eta = \frac{\lambda}{p},$$
$$\mathbf{q}_{nm} \equiv \boldsymbol{\kappa}_1-\boldsymbol{\kappa}_2-(n+2m)\mathbf{q}, \quad (14)$$

[2] It is useful to say that Voitkiv et al. denote by α_0 a different quantity (see [1], Eq. (11)).

where α is the fine structure constant and c the velocity of light, the matrix element O_{nm} has the expression

$$O_{nm} = N_0 Z_1 Z_2 Z_3,$$
$$Z_1 = \mathbf{q}_{nm}^2 - (i\eta + 1)\mathbf{p}\cdot\mathbf{q}_{nm}, \quad (15)$$
$$Z_2 = \left[\mathbf{q}_{nm}^2 + (\lambda - ip)^2\right]^{-i\eta-1},$$
$$Z_3 = \left[(\mathbf{q}_{nm} - \mathbf{p})^2 + \lambda^2\right]^{i\eta-2}, \quad (16)$$
$$|N_0|^2 = \frac{32}{\pi}\lambda^5 m_e \frac{\eta \exp(\pi\eta)}{\sinh(\pi\eta)} p. \quad (17)$$

Finally, we have to mention that for forward electron emission and linear polarization perpendicular to the electron momentum ($\xi = 180°$) the adopted approximation fails because the **r**-independent terms kept in (9) and (11) vanish.

4 Numerical results

We present only results for perpendicular laser and incident photon directions of propagation. Accordingly to our initial choice the reference frame has the y-axis along the laser propagation direction. The z-axis was taken along the incident photon direction. The results presented in the figures refer to atomic hydrogen.

We have studied two quantities: (i) the most differential cross-section corresponding to the detection in coincidence of the scattered photon of given frequency and direction with the electron direction and (ii) the electron energy distribution at fixed electron direction, for any scattered photon attributes. As mentioned before, the numerical calculation is simpler in the case of circular laser polarization because in this case only the matrix elements O_{n0} [see definition (13)] appear. We have developed codes for the calculation of the cross-sections for arbitrary polarization of the laser. Having in mind the remark at the end of Section 3 about the validity of the analytic expressions we use, we do not present results for $\xi > 150°$.

Due the monochromaticity of the external field, the fully differential electron spectrum is a succession of lines. So, at given scattered frequency, the energy of the electron can have the discrete values allowed by the δ-function in (3),

$$E_e^n = \hbar\omega_1 - \hbar\omega_2 + E_1 - n\hbar\omega_{\rm L} - U_{\rm P}, \quad (18)$$

corresponding to the absorption ($n < 0$) or emission of laser photons ($n > 0$). The number of emitted photons is limited by the condition $E_e^n > 0$. The quantity investigated in this case is

$$\sigma_3(E_e) = \sigma_{\rm Th}\frac{\omega_2}{\omega_1}|M_{fi;n}|^2 \quad (19)$$

for different values of the energy E_e, as given by (18). The result is a figure as Figures 1 and 2 here, of the type of Figure 1 of [1]. We shall call the content of such a figure *the electron spectrum.*

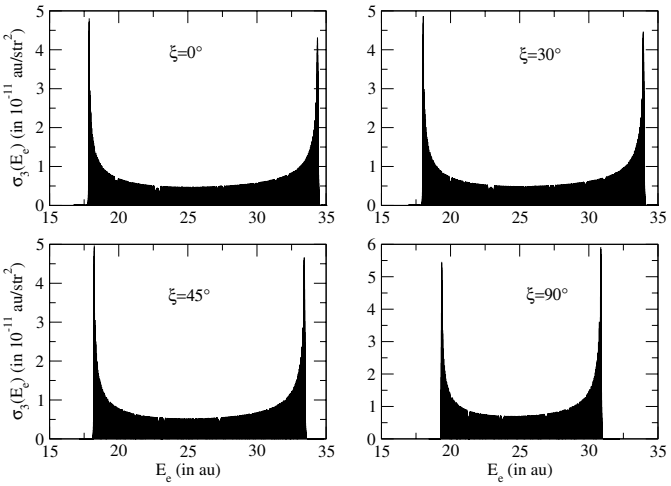

Fig. 1. The electron spectrum (19) for 500 au incident photon energy, backward scattered photon with 475 au energy and forward emitted electron. The laser parameters are $F_0 = 0.005$ au and $\omega_{\rm L} = 0.0043$ au. The laser polarization ellipticity ξ changes from a panel to another.

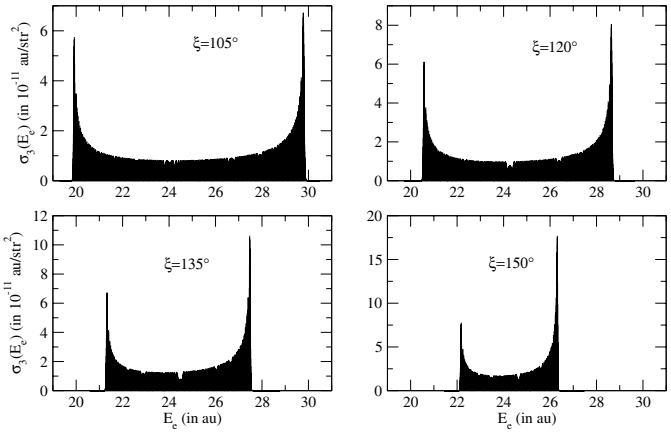

Fig. 2. Same as Figure 1, but for other degrees of laser polarization.

In the absence of the laser field the electron spectrum reduces to a single line. The intensity of this unique line is maximum for backward photon scattering, forward electron emission and a scattered frequency close to the free-electron Compton frequency. In the presence of the external electromagnetic field the spectrum is extremely rich, hundreds of lines are present in Figures 1 and 2.

We have studied the change of the spectrum with some of the parameters it depends on. We summarize our observations, that show a similar qualitative behaviour as that of the single line present in the absence of the field.

(1) For electron emitted along the incident photon direction ($\theta_e = 0$) the spectrum does not depend on the azimuthal angle ϕ_2 of the scattered photon. The conclusion is based on the analytic expression of the cross-section.

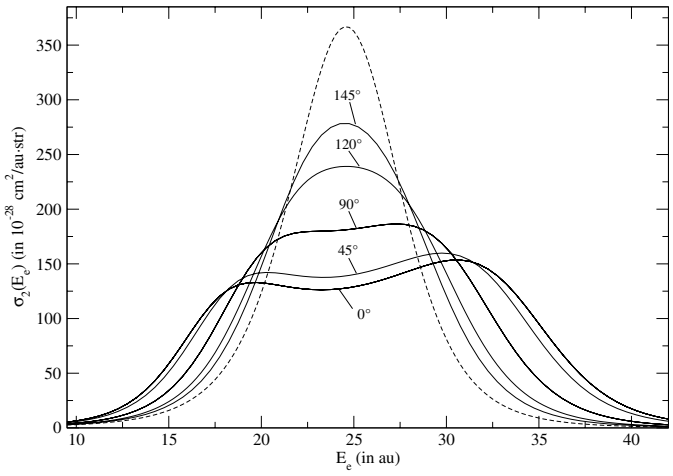

Fig. 3. The cross-section (20) for different values of the ellipticity ξ, at 500 au incident photon energy and forward emitted electron, laser parameters $F_0 = 0.005$ au and $\omega_L = 0.0043$ au. The dashed curve corresponds to the absence of the laser.

(2) At a given initial frequency ω_1 the lines have the largest intensities for the Compton frequency of the free electron.
(3) The effect of departure from forward electron scattering or from backward photon scattering is a drastic reduction of the spectrum.

The spectra shown in Figures 1 and 2 correspond to an incident photon frequency of $\omega_1 = 500$ au, the frequency of the laser $\omega_L = 0.0043$ au (the fundamental frequency of the CO_2 laser) and the laser electric field $F_0 = 0.005$ au. The other parameters (scattered photon frequency and direction, emitted electron direction) are those favorable to the Compton effect in the absence of the field, as described before. The laser polarization, characterized by the parameter ξ in (1), is changed from a panel to another. The Compton frequency for backward scattering is approximately 475 au, so the position of the line in the absence of the field would be at an electron energy of 24.8 au. Its intensity, not shown in these figures, is two, sometimes three orders of magnitude higher that the largest intensity in the laser modified spectrum. As shown in the figures, the spectrum is not symmetric with respect to the Compton frequency. The absorption of laser photons is favored for values of the ellipticity parameter ξ smaller than 90°. For circular polarization the spectrum is almost symmetric. The extension of the emitted electron energy range is reduced with the increase of the ellipticity: it is reduced from approximately 18 au for linear polarization to 4 au at $\xi = 150°$.

If the scattered photon is not detected, the integration of its attributes in equation (3) leads to the cross-section

$$\sigma_2(E_e) = \frac{d^2\sigma}{d\Omega_e dE_e} = \int d\Omega_2 \sum_{n=-\infty}^{n_0} |M_{fi;n}|^2, \qquad (20)$$

where n_0 denotes the maximum number of laser photons that can be emitted. The cross-section $\sigma_2(E_e)$ will be

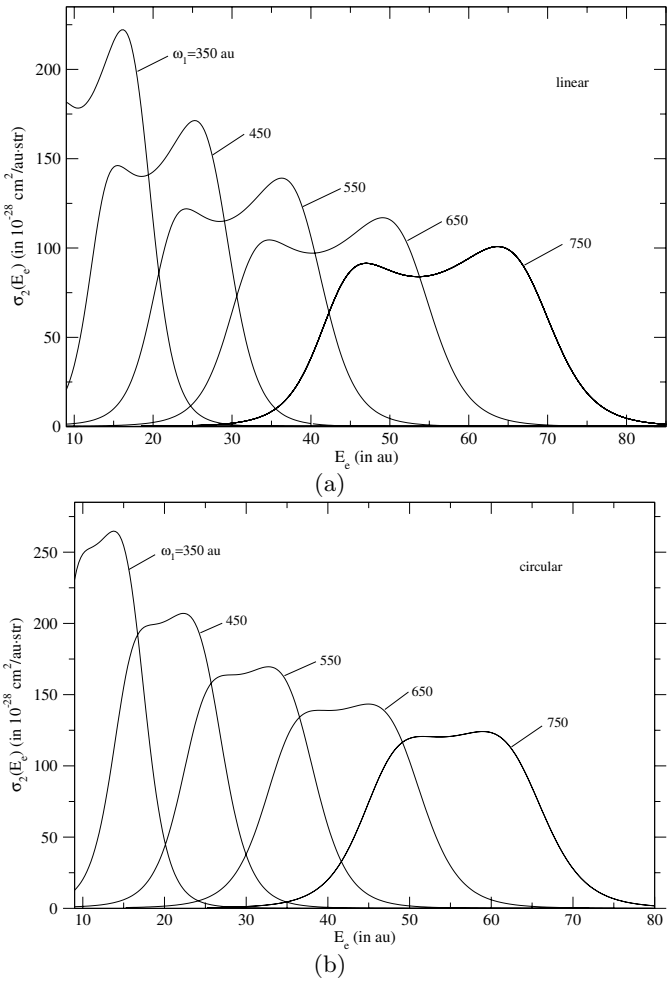

Fig. 4. The cross-section (20) for different incident photon energies, forward emitted electron and laser parameters $F_0 = 0.005$ au, $\omega_L = 0.0043$ au: (a) linear polarization; (b) circular polarization.

named the *electron energy distribution*. Besides the laser parameters, the electron energy distribution depends on the incident frequency and the electron direction.

The following figures (Figs. 3–5) are of the type of Figure 2 of [1], i.e., they represent the cross-section σ_2 as function of the final electron energy E_e. They correspond all to an incoming photon and emitted electron along the $z-$axis of the reference system.

As for $F_0 = 0.005$ au, $\omega_L = 0.0043$ au and $E_e = 10$ au one has already $\zeta = 0.35$, the electron energy range was restricted to $E_e > 10$ au. Nevertheless, in Figure 5 some higher, but smaller than 1, values of ζ are met at the intensity $F_0 = 0.01$. The reason to display this graph is to supply a term of comparison for more adequate calculations at higher laser intensities.

Figure 3 illustrates the dependence of the electron energy distribution on the laser polarization. The other laser parameters ω_L and F_0 are the same as in Figure 1, so are the scattered photon and emitted electron attributes. The dashed curve corresponds to the distribution in the

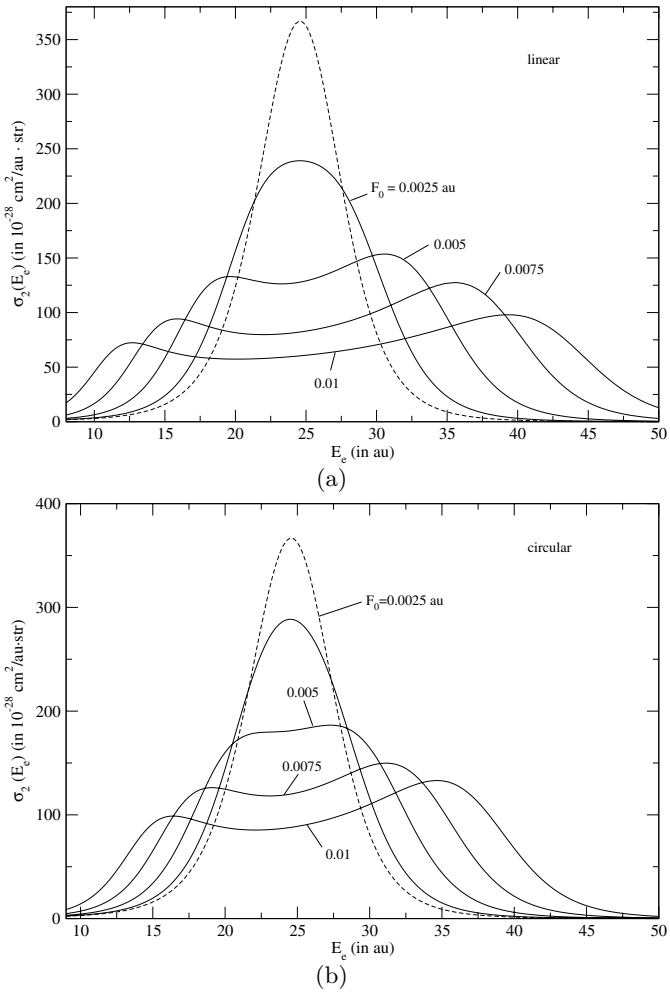

Fig. 5. The cross-section (20) for 500 au for different values of the laser electric field intensity F_0, laser frequency ω_L = 0.0043 au and forward emitted electron: (a) linear polarization; (b) circular polarization. The dashed curve corresponds to the absence of the laser.

absence of the laser field. The laser field influence is reduced by the increase of the ellipticity parameter ξ.

Results valid in the case of laser linear polarization ($\xi = 0$) along the incident photon direction (Figs. 4a and 5a) are compared with those for circular polarization (Figs. 4b and 5b). These results concern the dependency on the incident photon frequency which differs from a curve to another in Figures 4a and 4b and the dependence on the electric field intensity in Figures 5a and 5b, which is now changed from a curve to another.

As seen in Figures 4a and 4b, with the increase of the incident photon energy in the investigated range (350–750 au), the electron distribution changes its shape, in a similar way in the linear and circularly polarized laser field.

At low laser intensities the electron distribution keeps the shape it has in the absence of the laser field (the dashed curve), but at larger intensities it is deformed. The effect are more pronounced for linear polarization.

5 Conclusions

We have studied the influence of a low-frequency laser polarization on the sea-gull term in the amplitude of the Compton scattering on the electron in the ground state of a hydrogenic atom, using the approximation introduced by Voitkiv et al. and used by them in the circularly polarized case. We have found that the polarization degree does affect in a noticeable way the values of the cross-sections.

Further studies have to be concerned with the contribution of the other terms in the Compton scattering amplitude, starting from what is known in the absence of the field [17].

This work was partially supported by the Romanian CNCSIS grant 27694/8a/2005. We are grateful to Madalina Boca for competent assistance in the numerical calculation.

References

1. A.B. Voitkiv, N. Grün, J. Ullrich, J. Phys. B: At. Mol. Opt. Phys. **36**, 1907 (2003)
2. A.B. Voitkiv, N. Grün, J. Ullrich, J. Phys. B: At. Mol. Opt. Phys. **37**, 2641 (2004)
3. P.M. Bergstrom Jr, R.H. Pratt, Radiat. Phys. Chem. **50**, 3 (1997)
4. M. Gavrila, Phys. Rev. A **6**, 1348 (1972)
5. A. Costescu, M. Gavrila, Rev. Roum. Phys. **18**, 493 (1973)
6. A. Costescu, F.D. Aaron, I. Schneider, I.N. Mihailescu, Opt. Lett. **11**, 449 (1986)
7. P. Panek, J.Z. Kaminski, F. Ehlotzky, Eur. Phys. J. D **26**, 3 (2003)
8. M. Jain, N. Tzoar, Phys. Rev. A **18**, 538 (1978)
9. F. Ehlotzky, Phys. Lett. A **69**, 24 (1978)
10. P. Eisenberger, P.M. Platzman, Phys. Rev. A **2**, 415 (1970)
11. A.B. Voitkiv, J. Ullrich, J. Phys. B: At. Mol. Opt. Phys. **34**, 4383 (2001)
12. P. Cavaliere, G. Ferrante, C. Leone, J. Phys. B: At. Mol. Opt. Phys. **13**, 495 (1980)
13. J. Banerji, M.H. Mittleman, J. Phys. B: At. Mol. Opt. Phys. **14**, 3717 (1981)
14. N.M. Kroll, K.M. Watson, Phys. Rev. A **8**, 804 (1973)
15. A.S. Kornev, B.A. Zon, J. Phys. B: At. Mol. Opt. Phys. **35**, 2451 (2002)
16. F.H.M. Faisal, J. Phys. B: At. Mol. Opt. Phys. **38**, R1 (2005)
17. T. Suric, P.M. Bergstrom Jr, K. Pisk, R.H. Pratt, Phys. Rev. Lett. **67**, 189 (1991)